Phototransistor with nanocrystalline Si/amorphous Si bilayer channel

Cite as: Appl. Phys. Lett. **96**, 173507 (2010); https://doi.org/10.1063/1.3422479
Submitted: 19 February 2010 • Accepted: 10 April 2010 • Published Online: 30 April 2010

Yuri Vygranenko, Arokia Nathan, Manuela Vieira, et al.

Phototransistor with nanocrystalline Si/amorphous Si bilayer channel

Yuri Vygranenko,[1,a] Arokia Nathan,[2] Manuela Vieira,[1,3] and Andrei Sazonov[4]
[1]*Department of Electronics, Telecommunications and Computer Engineering, ISEL, P-1959-007 Lisbon, Portugal*
[2]*London Centre for Nanotechnology, University College London, London WC1H 0AH, United Kingdom*
[3]*CTS-UNINOVA, Quinta da Torre, P-2829-516 Caparica, Portugal*
[4]*Department of Electrical and Computer Engineering, University of Waterloo, Ontario N2L 3G1, Canada*

(Received 19 February 2010; accepted 10 April 2010; published online 30 April 2010)

We report a field-effect phototransistor with a channel comprising a thin nanocrystalline silicon transport layer and a thicker hydrogenated amorphous silicon absorption layer. The semiconductor and dielectric layers were deposited by radio-frequency plasma enhanced chemical vapor deposition. The phototransistor with channel length of 24 microns and photosensitive area of 1.4 mm^2 shows an off-current of about 1 pA, and high photoconductive gain in the subthreshold region. Measurements of the quantum efficiency at different incident light intensities and biasing conditions, along with spectral-response characteristics, and threshold voltage stability characterization demonstrate the feasibility of the phototransistor for low light level detection. [doi:10.1063/1.3422479]

There is significant interest in optical sensors whose fabrication process is fully compatible with existing flat panel display thin film transistor (TFT) technology. A hydrogenated amorphous silicon (*a*-Si:H) thin film phototransistor can serve as a sensing element in contact image sensors[1] or as an optical feedback element in active matrix organic light-emitting diode (LED) displays.[2] The most challenging application lies in nondirect conversion x-ray image sensor, for which low light level detection is required.[3]

The advantage of phototransistors over conventional *a*-Si:H *p-i-n* photodiodes or metal-insulator-semiconductor photosensors potentially lies in photoconductive gain. In the conventional *a*-Si:H transistor, however, the channel is too thin for efficient light absorption, and the light-to-dark current ratio is appreciable only in a narrow range of gate biases. Two device modifications such as a source-gated phototransistor,[4,5] and a thick-layered etched-contact phototransistor[1] have been proposed to increase the dynamic range and optical gain. In spite of a low mobility-lifetime product in *a*-Si:H ($\mu\tau$ typically about 10^{-7} cm^2/V), a high photoconductive gain can be achieved by reducing the channel length, while a large channel width limits pixel scaling and fill factor. The threshold voltage instability of *a*-Si:H transistors is also a limiting factor. Both these issues could be resolved with a superior electron transport channel material, such as nanocrystalline silicon (nc-Si:H).[6] However, it has a relatively low absorption coefficient, which serves to reduce the optical gain.[7] In this paper, we capture the advantages of both *a*-Si:H and nc-Si:H by using a bottom-gate phototransistor with a channel layer composed of a thin nc-Si:H film with a thicker *a*-Si:H layer on top. Here, the *a*-Si:H serves as a photosensitive layer whereas the function of the nc-Si:H layer is to transport the photogenerated carriers.

Figure 1 shows a cross-sectional view (a) and micrograph (b) of the phototransistor with the nc-Si:H/*a*-Si:H bilayer channel. This is a back channel passivated configuration, in which the silicon nitride (*a*-SiN_x:H) gate dielectric, channel, and *a*-SiN_x:H passivation layers are consecutively deposited in one-pump-down vacuum process. The *a*-Si:H absorption layer is chosen to be 80 nm thin, because a thicker layer would significantly increase source-drain contact resistance.[8] To enhance the optical gain, the thickness of the gate dielectric is designed for maximum backside reflection. Further, the fabrication sequence includes patterning by wet etching of the *a*-Si:H/*a*-SiN_x:H layers to form the channel islands, followed by deposition of a SiO_x layer. Here, the *a*-SiN_x:H/SiO_x bilayer serves as an antireflecting coating with an optical length of $3\lambda_o/4$, λ_o=550 nm. After patterning the *a*-SiN_x:H/SiO_x bilayer by wet etching, a n^+ *a*-Si:H/Al stack is deposited. Then, the Al layer is patterned and the n^+-layer is etched in SF_6 plasma using SiO_x as a stop-etch layer. All semiconductor and dielectric layers were

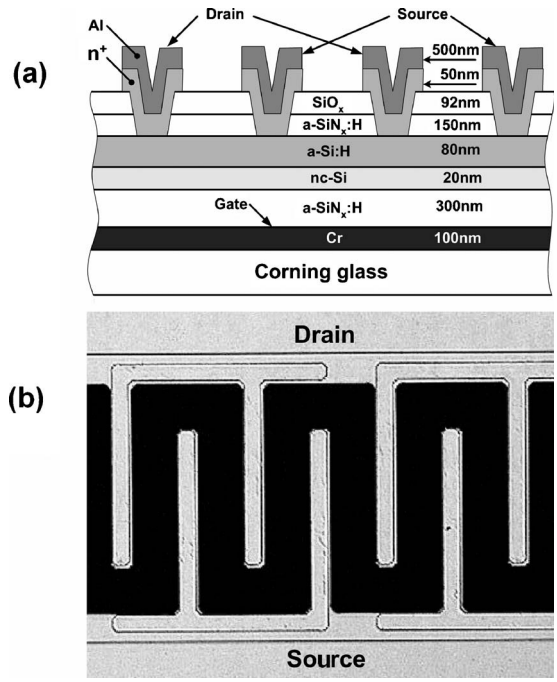

FIG. 1. (a) Cross-sectional view and (b) photomicrograph of phototransistor.

[a]Electronic mail: yvygranenko@deetc.isel.ipl.pt.

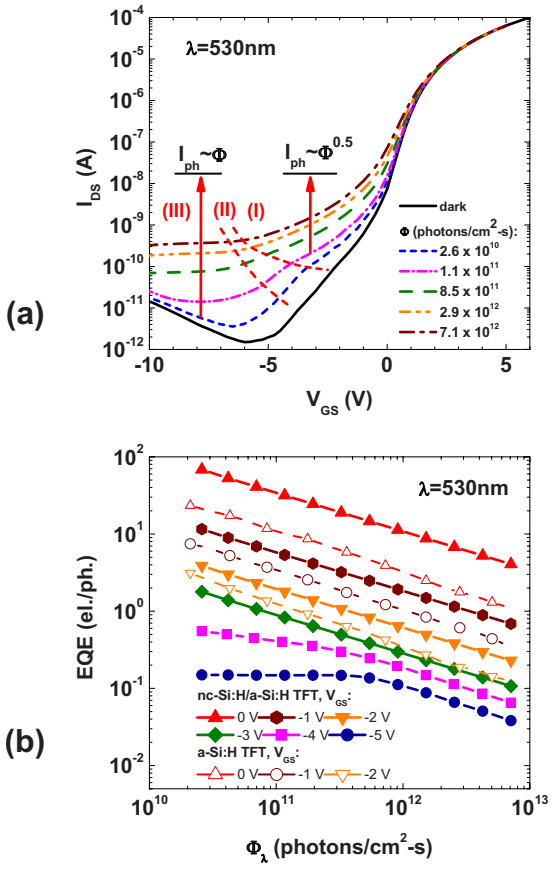

FIG. 2. (Color online) (a) Dark and ambient light transfer characteristics, and (b) EQE as a function of photon flux at $V_{DS}=5$ V.

deposited at 280 °C in a multichamber 13.56 MHz plasma enhanced chemical vapor deposition system. The nc-Si:H channel layer was deposited using silane source gas highly diluted in hydrogen at a 1:100 ratio. High film crystallinity, in excess of 60%, implying formation of crystalline grains at the early stages of film growth was confirmed by Raman measurements, while transmission electron microscope cross section of the deposited film showed no obvious presence of an amorphous incubation layer.[8] The deposition conditions for other layers have been reported elsewhere.[9]

The phototransistors reported in this work have a channel length of 24 μm and 64 pairs of source-drain finger-shaped contacts [see Fig. 1(b)]. The width and length of the contact are 12 μm and 80 μm, respectively. For high accuracy measurement purposes, a test structure comprising nine phototransistors connected in parallel yields a total photosensitive area of 1.4 mm^2. Using the same photolithography mask set, phototransistors without the nc-Si layer have been also fabricated for comparison.

Figure 2(a) shows quasistatic dark and light transfer characteristics of the nc-Si:H/*a*-Si:H phototransistor array at a source-drain voltage (V_{SD}) of 5 V. A field-effect mobility of 0.28 cm^2/V s, and a threshold voltage of 2.4 V were obtained from the above-threshold region of the dark I_{DS}-V_{GS} characteristic. The subthreshold slopes of the log $|I_{DS}|-V_{GS}$ curve are 0.52 and 1.51 V/dec, determined between 0 and 0.8 V in the forward subthreshold region (conduction at the nc-Si:H/*a*-SiN$_x$:H interface), and between −1 and −4.5 V in the reverse subthreshold region (conduction at the *a*-Si:H/*a*-SiN$_x$:H interface), respectively. The dark current

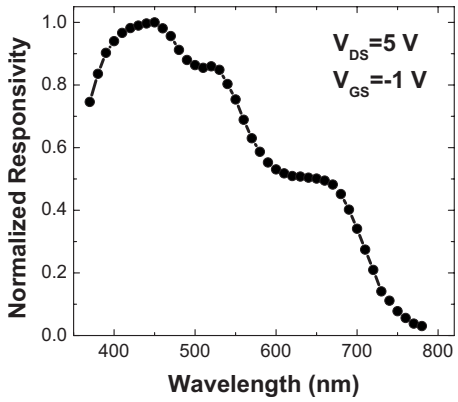

FIG. 3. Spectral-response characteristics of the phototransistor.

reaches a minima of 1.6 pA at a gate bias of −6 V and exponentially increases at high negative gate voltages due to the Poole–Frenkel field-enhanced thermionic emission at the gate–drain overlap vicinity.[10]

Analyzing the relation between the photocurrent and the incident light intensity, we define three regimes of device operation. In regime (I), which takes place in the forward subthreshold region and partially in the reverse subthreshold region, the drain current follows the dependence

$$I_{DS} = I_{DSdark} + I_{DSph} = I_{DSdark} + q\,\eta_{opt} G A \Phi_\lambda{}^{\gamma}, \tag{1}$$

where I_{DSdark} is the dark current component, I_{DSdark} is the photocurrent, q is the elementary charge, η_{opt} is the optical gain, G is the photoconductive gain, A is the photosensitive area, Φ_λ is the incident photon flux density, and γ is a parameter evaluated to be 0.5 ± 0.03 for the investigated device. In the transition regime (II), γ varies from 0.5 to 1 in a narrow bias range. In regime (III), hole accumulation at the nc-Si:H/*a*-SiN$_x$:H interface leads to formation of *p*-*n* junctions at the source and drain, which are in the ON- and OFF-states, respectively. Consequently, the current is limited only by photogeneration of electron and holes at the drain *p*-*n* junction depletion region, and the photocurrent becomes proportional to the photon flux analogous to that in a photodiode.[11] The corresponding external quantum efficiency (EQE) values are depicted in Fig. 2(b) as a function of photon flux density for different gate biases. The EQE curves of the photodiode with an *a*-Si:H channel layer are also shown here for comparison. The measurements were performed at $V_{DS}=5$ V on a wavelength of 530 nm. The nc-Si:H/*a*-Si:H phototransistor exhibits a high photoconductive gain at low photon fluxes in regime (I). Here, the EQE is proportional to $\Phi_\lambda{}^{-0.5}$ (curves at $V_{GS}=-3$; −2; −1, and 0 V). In regime (II) (curve at $V_{GS}=-4$ V), the EQE is lower than unity. In regime (III) at $V_{GS}=-5$ V, the EQE saturates at a value of 0.15. The *a*-Si:H phototransistor shows a factor of 3 lower EQE values at zero gate bias, while at negative gate biases, when the electron transport via the *a*-Si:H layer bulk becomes dominant, the difference in EQE is lower. Thus, the nc-Si:H/*a*-SiN$_x$:H interface exhibits better transport properties yielding higher photoconductive gain in comparison to the device with the *a*-Si:H channel.

Figure 3 shows the spectral response of the nc-Si:H/*a*-Si:H phototransistor measured at $V_{GS}=-1$ V and $V_{DS}=5$ V. The measurements were performed using a lock-in technique at a light modulation frequency of 12 Hz.

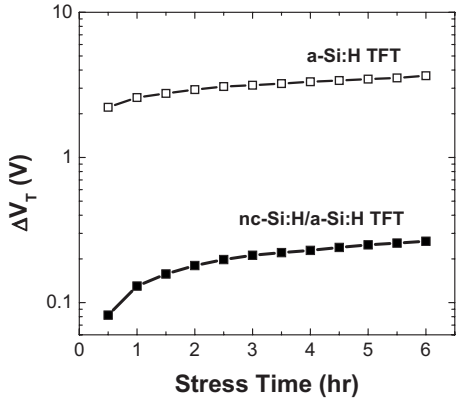

FIG. 4. Time dependence of the threshold voltage shift of nc-Si:H and *a*-Si:H TFTs under constant gate-bias stress.

To avoid spectral distortion, a green LED was used to create background illumination of 10^{12} photons/cm^2, while the intensity of the modulated light was at least ten times lower. The spectral responsivity increases with decreasing wavelength due to increasing absorption in the *a*-Si:H, and reaches a maximum at a wavelength of 450 nm. At shorter wavelengths, recombination at the *a*-Si:H/*a*-SiN$_x$:H interface becomes a limiting factor.

To examine device stability, long-term bias-stress experiments were performed for the nc-Si:H/*a*-Si:H and *a*-Si:H TFTs having the same geometry. Both devices were subjected to constant gate bias stress of $V_{GS}-V_T=10$ V. The source and drain were grounded in order to create a uniform electric field across the channel interface. At every 30 min intervals, the stress test was interrupted to retrieve transfer characteristics of the TFT for device parameter extraction. The total stress time was stretched to 6 h. Figure 4 shows the threshold voltage shift (ΔV_T) as a function of stress time for the tested devices. After a stress time of 6 h, ΔV_T values for nc-Si:H and *a*-Si:H devices are 0.265 V and 3.66 V, respectively. The enhanced threshold voltage stability observed has also been reported for nc-Si:H TFTs stressed at constant drain currents.[12] These results further corroborate absence of defect state creation in the nc-Si:H TFTs at low light levels.

In conclusion, bottom-gate phototransistors with the nc-Si/*a*-Si:H channel bilayer show a photoconductive gain over unity and leakage current of the order of picoamperes under optimized biasing conditions. Spectral response and linearity measurements along with device stability evaluation demonstrate the feasibility of the phototransistor for low light level detection.

[1]S. GadelRab and S. Chamberlain, IEEE Trans. Electron Devices **45**, 465 (1998).
[2]D. A. Fish, N. D. Young, S. Johan, H. J. Cornelissen, and S. C. Deane, U.S. Patent Application No. 20100053045 A1 (pending).
[3]*Technology and Applications of Amorphous Silicon*, edited by R. A. Street (Springer, New York, 2000).
[4]Y. Kaneko, N. Koike, K. Tsutsui, and T. Tsukada, Appl. Phys. Lett. **56**, 650 (1990).
[5]S. M. GadelRab and S. G. Chamberlain, IEEE Trans. Electron Devices **44**, 1789 (1997).
[6]C.-H. Lee, A. Sazonov, A. Nathan, and J. Robertson, Appl. Phys. Lett. **89**, 252101 (2006).
[7]M. R. Esmaeili-Rad, A. Sazonov, A. G. Kazanskii A. A. Khomich, and A. Nathan, J. Mater. Sci.: Mater. Electron. **18**, 405 (2007).
[8]M. R. Esmaeili-Rad, A. Sazonov, and A. Nathan, J. Appl. Phys. **103**, 074502 (2008).
[9]A. Sazonov, D. Striakhilev, C.-H. Lee, and A. Nathan, Proc. IEEE **93**, 1420 (2005).
[10]A. Nathan, A. Kumar, K. Sakariya, P. Servati, K. S. Karim, D. Striakhilev, and A. Sazonov, IEEE J. Sel. Top. Quantum Electron. **10**, 58 (2004).
[11]*Thin-Film Transistors*, edited by C. R. Kagan and P. Andry (Marcel Dekker, New York, 2003).
[12]M. R. Esmaeili-Rad, A. Sazonov, and A. Nathan, Appl. Phys. Lett. **91**, 113511 (2007).